Translational Stroke Research (2019) 10:150–159
https://doi.org/10.1007/s12975-018-0629-8

ORIGINAL ARTICLE

Enriched Environment Elicits Proangiogenic Mechanisms After Focal Cerebral Ischemia

Hongyu Xie[1,2] · Kewei Yu[1,2] · Naiyun Zhou[3] · Xueyan Shen[1,2] · Shan Tian[1,2] · Bei Zhang[1,2] · Yuyang Wang[1,2] · Junfa Wu[1,2] · Gang Liu[1,2] · Congyu Jiang[1,2] · Ruiping Hu[1,2] · Cenk Ayata[4] · Yi Wu[1,2]

Received: 18 October 2017 / Revised: 1 March 2018 / Accepted: 29 March 2018 / Published online: 26 April 2018

Abstract

Brain has limited capacity for spontaneous recovery of lost function after stroke. Exposure to enriched environment (EE) can facilitate functional recovery, but mechanisms underlying this effect are poorly understood. Here, we used a middle cerebral artery occlusion (MCAO) model to investigate the impact of EE on angiogenesis in the post-ischemic brain in adult male Sprague Dawley rats, and examined whether blood-borne factors may contribute. Compared with standard cage (SC), exposure to EE was associated with greater improvement in neurological function, higher peri-infarct vascular density, and higher chronic post-ischemic cerebral blood flow assessed by laser speckle imaging. The effect persisted for at least 28 days. EE also enhanced the expression of hepatocyte growth factor in the peri-ischemic cortex when measured 15 days after MCAO. Interestingly, serum from rats exposed to EE after MCAO showed elevated levels of hepatocyte growth factor, and plasma or serum from rats exposed to EE after MCAO enhanced the survival and proliferation of cultured endothelial cells, in vitro, when compared with control plasma or serum from SC group after MCAO. Together, our data suggest that exposure to EE promotes angiogenesis in the ischemic brain that may in part be mediated by blood-borne factors.

Keywords Enriched environment · Cerebral ischemia · Angiogenesis · Cerebral blood flow · Hepatocyte growth factor

Introduction

Stroke is a major cause of disability [1, 2]. Therapies targeting neurological recovery after stroke can impact a much larger population of patients than those eligible for acute stroke interventions. Harnessing endogenous pathways is a promising but underexplored avenue to promote recovery after stroke [3]. Angiogenesis is an innate repair response to restore tissue oxygen and glucose delivery after ischemic stroke, and to provide trophic support to newly generated neurons [4–7]. Post-stroke angiogenesis improves tissue perfusion, and endothelial cells release a plethora of neurotrophic factors, supporting the activity of neurons and progenitor cells to enhance functional recovery. Clinically, greater microvessel density in the ischemic border correlates with longer survival in stroke patients [8]. Thus, post-stroke angiogenesis is an important target for therapeutic interventions.

Enriched environment (EE) is one way to recruit endogenous pathways to promote recovery. It has been consistently shown that EE facilitates neurological recovery after cerebral ischemia in different paradigms [9–11]. EE also promotes endothelial cell proliferation in adult rat hippocampus and prefrontal cortex [12]. In this study, we aimed to determine whether exposure to EE can promote angiogenesis and blood flow in the post-ischemic brain and neurological recovery after stroke, and examined potential mechanisms. Our results suggest that EE enhances angiogenesis in the ischemic brain, and blood-borne factors may play a role.

Hongyu Xie and Kewei Yu contributed equally to this study.

✉ Cenk Ayata
cayata@partners.org

✉ Yi Wu
wuyi@fudan.edu.cn

[1] Department of Rehabilitation Medicine, Huashan Hospital, Fudan University, WuLuMuQi Middle Road 12, Shanghai 200040, China

[2] State Key Laboratory of Medical Neurobiology, Fudan University, Shanghai 200040, China

[3] Department of Biomedical Engineering, Stony Brook University, New York, USA

[4] Neurovascular Research Laboratory, Department of Radiology, Massachusetts General Hospital, Harvard Medical School, 149 13th Street, Room 6403, Charlestown, MA 02129, USA

Methods

Experimental Animals

All experimental procedures were carried out in accordance with the ARRIVE guidelines, and the Guide for Care and Use of Laboratory Animals (NIH publication no. 85–23, 1996), and were approved by the institutional review board. Adult male Sprague Dawley rats (7- to 8-week old, 250–270 g for in vivo experiments and 2- to 3-day old, 50–60 g for in vitro experiments, Shanghai SLAC Laboratory Animal, Co., Ltd.) were used as subjects. All rats were housed under a 12-h light/dark cycle, with food and water available ad libitum throughout the study.

Transient Focal Cerebral Ischemia

The left middle cerebral artery occlusion (MCAO) was performed as previously described [13]. Briefly, rats were anesthetized with 1.5% isoflurane (Abbott, USA) in room air. The left femoral artery was cannulated to monitor systemic arterial blood pressure, pH, pO_2, and pCO_2 (ABL505, Radiometer, Copenhagen, Denmark, Table 1). Rectal temperature was maintained at 37.0 °C by a thermostat-controlled heating blanket. After a midline cervical incision, the left common carotid artery was exposed, and the external carotid artery ligated distally. To occlude the origin of the middle cerebral artery, a 4-0 nylon monofilament with a silicone tip was inserted through the external carotid into the internal carotid artery and advanced 1.9–2.0 cm from the bifurcation site. Peri-ischemic cerebral blood flow (CBF) changes were examined by laser speckle imaging (see below). After 90 min, reperfusion was established by withdrawal of the filament. For the sham control group, all steps were included, except for the insertion of the filament into the carotid artery. A total of 19 rats died prior to group allocation. One rat was excluded per protocol due to lack of neurological deficits after MCAO.

Housing Conditions

One day after transient MCAO, rats were randomly assigned to one of the following groups: sham, EE, or standard cage (SC). EE rats were generally housed in groups of six rats per cage in large cages (120 × 80 × 100 cm) containing various objects (e.g., boxes, chains, metal barrels, ladders, toy, running wheels, etc.) that were changed daily to maintain the activity level of rats (Fig. 1a), as described previously [14]. Exposure to EE started 1 day after MCAO and continued for 28 days. Rats were placed in EE 6 h a day (9:00 a.m. to 3:00 p.m.), and kept in a SC outside this time window. Control rats were housed in SC in groups of four rats per cage for 28 days (40 × 30 × 20 cm) that were devoid of objects (Fig. 1b). Sham-operated rats were also kept in standard cages similar to control rats. The EE protocols employed in previous studies, and their impact on stroke outcome, have been highly variable [15]. To standardize the enrichment procedure, we quantified the locomotor activity (distance moved) during the 6-h spent in the EE or standard cage daily by tracking the movement of color-coded rats using an automated system (EthoVision XT 7.0, Noldus Information Technology) [16].

Neurological Assessment

Coordinated locomotor movement of the rat forelimbs was assessed in the "foot fault test" as previously described with some modifications [17]. Briefly, all rats were trained for 4 consecutive days before MCAO on a horizontal ladder with a regular arrangement of rungs (at 2-cm intervals). The test was performed 1 day before and 7, 14, 21, and 28 days after MCAO. All animals were trained and tested two times per session and every session was videotaped for quantification of forelimb placement (only consecutive steps were analyzed) as follows: score 0, total miss, the limb completely missed the rung; score 1, deep slip, the forelimb was placed on the rung, but slipped off and caused a fall; score 2, slight slip, the forelimb was placed on a rung, and then slipped off but did not result in a fall and the rat continued with a coordinated gait; score 3, replacement, the forelimb was placed on a rung, but then quickly lifted and placed on another rung before it was weight bearing; score 4, correction, the forelimb aimed for one rung, but was placed on another rung before touching the first one; score 5, partial placement, the forelimb was placed on the rung with wrist digits; score 6, correct placement, the forelimb was placed on the rung correctly. A blinded investigator analyzed videotapes. The scores of the two trials were averaged for analysis.

Forelimb use and asymmetries in postural weight support during exploratory activity was assessed by using cylinder test as described previously [14]. The animals were not trained before ischemia. The test was performed 1 day before and 3, 5, 7, 14, 21, and 28 days after MCAO. The rat was placed in a transparent plexiglas cylinder (diameter, 20 cm; height, 20 cm) and videotaped for 5 min. As the animal reared to explore the environment, the number of bilateral paw placements, placements of the paw ipsilateral to the lesion (left), and placements of the paw contralateral to lesion (right) were counted. Videotapes were analyzed in slow motion. Forepaw (left/right/both) use was recorded during the first contact against the cylinder wall after rearing and during lateral exploration. Left (ipsilateral) forepaw preference was expressed as a relative proportion of right forepaw contacts, and calculated as: (left − right)/(left + right + both) × 100%.

Spatial learning and memory was examined using water maze as described previously [18] with some modifications. Briefly, the water maze was a black-colored circular pool (2 m

Table 1 Systemic physiological parameters

	SC			EE		
	Baseline	During MCAO	Reperfusion	Baseline	During MCAO	Reperfusion
pH	7.39 ± 0.03	7.36 ± 0.07	7.40 ± 0.09	7.35 ± 0.04	7.32 ± 0.05	7.37 ± 0.05
pCO_2 (mmHg)	38 ± 3	48 ± 8	40 ± 7	41 ± 4	44 ± 9	38 ± 8
pO_2 (mmHg)	93 ± 4	88 ± 7	90 ± 6	94 ± 4	88 ± 5	92 ± 4
MABP (mmHg)	89 ± 4	94 ± 11	85 ± 10	86 ± 5	96 ± 5	89 ± 7

Data are mean ± standard deviation (SD). $p > 0.05$ SC vs. EE ($n = 18$ each)

MABP, mean arterial blood pressure; *SC*, standard condition; *EE*, enriched environment; *MCAO*, middle cerebral artery occlusion

in diameter) filled with water (temperature was 21–23 °C) with black dye to contrast white rats, and situated in a room with salient visual cues (Fig. 1e). Acquisition of spatial learning started at post-MCAO day 29 through day 32 for 4 consecutive days. Each animal received eight consecutive trials (with randomly assigned starting positions) per day to locate the platform submerged 2-cm beneath the water surface. They were allowed 60 s to locate the platform that was kept in a constant location. If they failed to locate the platform within 60 s, the rat was manually guided to the platform and remained there for 10 s. The mean escape latency per day was recorded for each animal. One day after the final acquisition training session (day 33 post MCAO), all rats performed a probe test with the escape platform removed. The animals

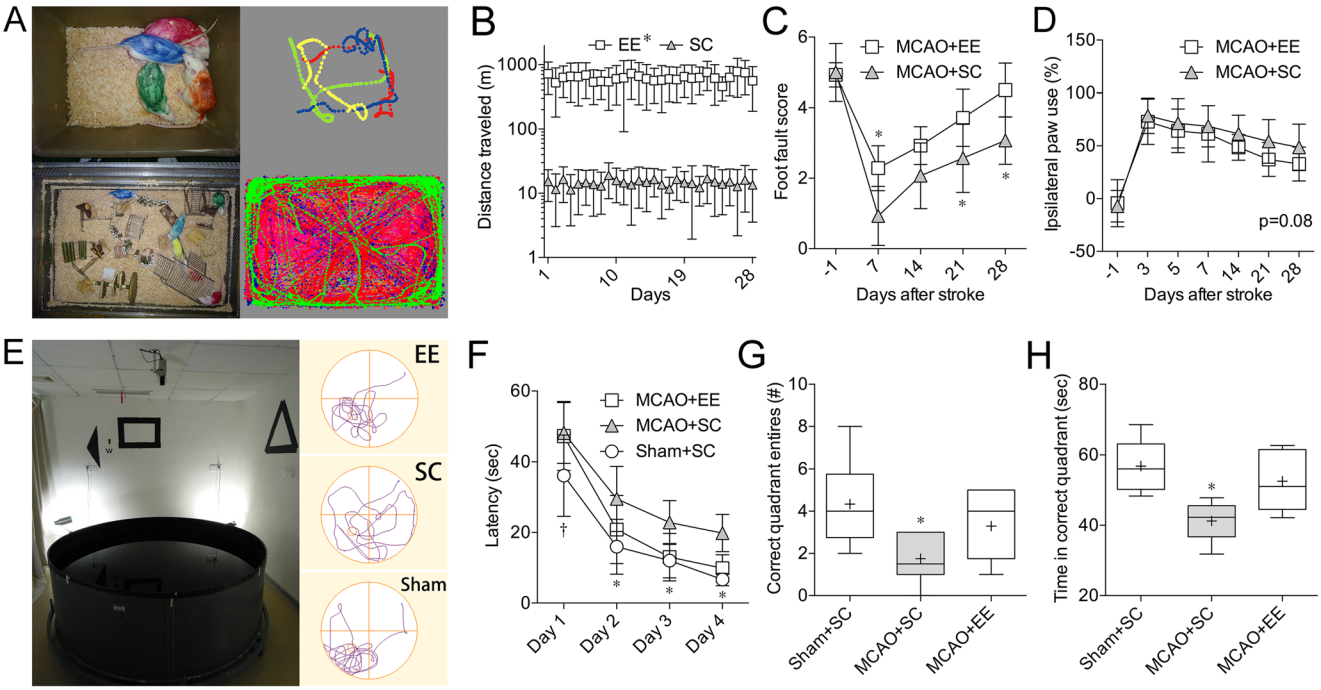

Fig. 1 Impact of EE on physical activity and neurocognitive function. **a** Computerized monitoring of the activity levels in standard cage and enriched environment was achieved by color coding the rats. The left panel shows the camera view and the right panel shows the movement path for each rat over the monitoring period. **b** Total distance moved by EE rats was significantly higher than SC rats during the 28-day observation period ($n = 12$ each; $^*p < 0.001$ vs. SC; two-way ANOVA for repeated measures followed by Sidak's multiple comparisons test). Note the logarithmic vertical scale. **c** Enriched environment (MCAO + EE) improved foot fault test performance throughout the 28-day recovery period ($n = 7$ each; $^*p < 0.05$; two-way ANOVA for repeated measures followed by Sidak's multiple comparisons test). **d** Enriched environment (EE) tended to improve cylinder test performance throughout the 28-day recovery period ($n = 7$ each; $p = 0.08$ vs. MCAO + SC; two-way ANOVA for repeated measures followed by Sidak's multiple comparisons test). **e** Water maze setup with spatial cues and automated camera system (left) to track rat's movement towards the target quadrant (right). **f** Latency to find the platform during the acquisition phase was significantly faster in EE rats ($n = 6$, 8, and 10 in Sham + SC, MCAO + SC, and MCAO + EE groups, respectively; $^*p < 0.05$ MCAO + SC vs. MCAO + EE and Sham + SC, $\dagger p < 0.05$ Sham + SC vs. MCAO + SC and MCAO + EE; two-way ANOVA for repeated measures followed by Tukey's multiple comparisons test). **g** The number of entries into the correct quadrant was significantly higher in EE ($^*p < 0.01$ vs. MCAO + EE and Sham + SC; one-way ANOVA followed by Tukey's multiple comparisons test). **h** Time spent in the correct quadrant was also longer in the EE group ($^*p < 0.05$ vs. Sham + SC; one-way ANOVA followed by Tukey's multiple comparisons test)

were placed into the pool from the location most distal to the target quadrant (with removed platform). The percent of time spent in the target quadrant and the number of times entered the platform area were recorded and interpreted as spatial memory.

Cerebral Blood Flow Measurement by Laser Speckle Imaging

Laser speckle imaging (LSI) was performed as previously described [19]. Under chloral hydrate anesthesia (10%, 0.36 mL/kg i.p.), head was fixed on a stereotaxic apparatus (David Kopf Instruments, Tujunga, CA, USA), scalp reflected and periosteum removed. Both parietal bones were thinned to translucency under saline cooling (12 × 10 mm) using a high-speed drill (Fine Science Tools, North Vancouver, Canada). Rat was then placed under a macro lens (Nikon 60 mm f/2.8 AF-S, Nikon Inc., Melville, NY, USA), and aperture was adjusted to match the speckle size to the area of a single pixel in a 12-bit CCD camera (270XS 11,066, Pixel fly, PCO, Kelheim, Germany). Shutter speed was set to an exposure time of 5 ms and images were continuously acquired at a rate of 23 frames per second. Imaging field was positioned to include both hemispheres. A 785-nm laser beam (L785P025, Visible Laser Diodes, Thorlabs China) was used to illuminate the thinned parietal bone surface in a diffuse and uniform manner. After acquiring baseline images (100 consecutive frames), rats were removed from the frame and transient filament MCAO was induced for 90 min as described above. Rats were then repositioned in the stereotaxic frame and LSF restarted at approximately 30 min after MCAO onset and continued for 15 min (50 consecutive sets of 100 consecutive frames of raw speckle images). Imaging session (15 min) was repeated 4 weeks later after once again thinning the parietal bone to translucency. Each experimental group had 7–14 animals. Analysis of laser speckle images was performed using MATLAB 7.0 software (Mathworks, MA, USA). In order to increase signal-to-noise ratio, 100 sequential raw speckle images were stacked and averaged to form one speckle contrast image. Because the spatial distribution of infarct slightly differed among animals, we placed a wide region of interest (ROI; 5 × 5 mm) at the approximate ischemic border zone (centered at 2.5 mm posterior, 2.5 mm lateral to bregma). Within this ROI, the $sp = 1/k^2$ was calculated [20], which is proportional to the velocity of red blood cells, and used as a surrogate for cerebral blood flow (CBF) [21, 22]. A blinded investigator performed all measurements. Because LSI can be confounded by differences in laser intensity and angle, and background light during individual imaging sessions, we standardized the $1/k^2$ values obtained at different time points by positioning a catheter (PE-50, 0.58 mm inner diameter) in the imaging field perfused with a polystyrene microsphere suspension via a perfusion pump (Thorlabs) at a constant velocity (1.9 mm/s). This served as an external reference standard for the tissue contrast values (k). CBF at different time points was normalized as $sp = [(k_1/k_2)\ [2]]sp$. In our prior experience where LSI was carried out and CBF was quantified during MCAO simultaneously with laser Doppler flowmetry in ischemic core, a 42 ± 15% residual CBF by LSI corresponded to 22 ± 6% residual CBF by laser Doppler (data not shown).

Western Blotting

Protein was extracted from ipsilateral cortical tissue 15 days after stroke. Western blots were performed as previously described [23]. Extracted protein (40 mg) was separated by 15% sodium dodecyl sulfate-polyacrylamide gel electrophoresis and transferred to polyvinylidene difluoride membranes at 350 V for 2.5 h with a cold pack. Membranes were incubated in a 5% bovine serum albumin blocking solution for 1 h at room temperature (RT), immersed overnight at 40 °C in anti-HGF antibody (1:500 dilution; cell signaling), incubated in horseradish peroxidase-labeled anti-rabbit secondary antibody for 1 h at RT with blocking buffer to detect immunoreactivity, developed using an ECL kit according to the manufacturer's instructions (Amersham Pharmacia Biotech, Freiburg, Germany), and then exposed to Kodak film for 5 to 30 s. Glyceraldehyde 3-phosphate dehydrogenase (GAPDH) was used as a loading control. Band intensities (optical density [OD] values) were quantified using Image J.

Elisa

Blood was allowed to clot for 2 h at room temperature, and centrifuged for 20 min at 1000 g. Serum HGF levels were measured using rat HGF ELISA (Cusabio Biotech Co., USA). One hundred microliters of serum was added per well and incubates for 2 h at 37 °C. After removing the liquid in each well, 100 μl of Biotin-antibody (1 ×) was added to each well and incubates for 1 h at 37 °C. Each well was then aspirated and washed three times. One hundred microliters of HRP-avidin (1 ×) was added to each well, incubated for 1 h at 37 °C, aspiration/wash was repeated for five times. Then, 90 μl of TMB substrate was added to each well, incubated for 15–30 min at 37 °C protecting from light, followed by adding 50 μl of stop solution to each well and reading at 450 nm within 5 min.

Vascular Labeling and Analysis of Vascular Density

Fluorescein isothiocyanate (FITC)-dextran (20kD, Sigma; 1 mL of 50 mg/mL) was administered intravenously 15 days after MCAO. The dye was allowed to circulate for 1 min. Rats were sacrificed by decapitation under general anesthesia. Brains were rapidly removed and placed in 4%

paraformaldehyde at 4 °C for 48 h. Ten 50-μm-thick coronal brain sections were cut at 1-mm intervals using a vibratome. Brain sections were analyzed with a laser-scanning confocal imaging system. Four cortical and four subcortical square regions of interest (200 × 200 μm) were placed within 1 mm of the infarct edge at the coronal level 0.8 mm anterior to bregma [24], by an investigator blinded to the experimental groups. The microvascular area was expressed as percentage of the total area (Image Pro Plus).

Measurement of Tissue Loss

Serial coronal cryosections were obtained between 1.4 and 4.8 mm posterior to bregma, were stained in 0.1% cresyl violet solution for 10 min at room temperature, and followed by quick differentiation in 1% glacial acetic acid (in 70% ethanol). Sections were then dehydrated and clarified through ethanol and xylene, respectively, and mounted with neutral balsam. Ipsilateral and contralateral hemispheric areas were then measured and integrated by an investigator blinded to experimental groups using Image J (NIH).

Oxygen-Glucose Deprivation in Rat Brain Microvascular Endothelial Cells

In accordance with previous methods [25, 26], cerebral gray matter from male Sprague Dawley rats (50–60 g) was chopped, homogenized, and passed through 200 and 80 μm mesh screens. Tissue remaining on the 80-μm mesh screen was digested with a 0.1% collagenase/dispase solution for 20 min at 37 °C, followed by centrifugation. Precipitate was incubated in complete culture medium, consisting of high-glucose Dulbecco's modified eagle medium (DMEM), supplemented with 20% fetal bovine serum (FBS), 100 μg/mL heparin, 100 μg/mL endothelial cell growth supplement, 3.75 mg/mL HEPES, 0.2 U/mL insulin, 0.3 mg/mL L-glutamine, 100 U/mL penicillin, and 100 μg/mL streptomycin, pH 7.2–7.4. rBMECs were employed at the second passage with 95% purity. We then coated 24-well cell culture plates evenly with Matrigel (BD Biosciences), incubated at 37 °C for 30 min, seeded rBMECs onto Matrigel-coated plates in culture media containing 2% FBS, incubated at 37 °C. After 18 h, capillary-like structures formed [27]. We analyzed the viability of rBMECs after oxygen/glucose deprivation (OGD) using the WST-8 assay with the Cell Counting Kit-8 (CCK-8, Dojindo Laboratories, Kamimashiki-gun, Kumamoto, Japan) [28]. For OGD, cells were incubated in glucose- and sodium pyruvate-free Dulbecco's modified eagle medium (DMEM; not supplemented with FBS) and 5% CO_2/95% N_2 (*v*/v) for 2 h in an airtight container. Then, cells were switched to high-glucose DMEM with EE or SC plasma for 24 h. Then CCK-8 solution was added to culture media (*v*/v 10:1), incubated for 4 h at 37 °C, and cell viability quantified by optical density (OD) at 450 nm using a spectrophotometer. To obtain plasma, blood samples were collected by ventricular puncture 1 day after the 28-day housing intervention. Blood was anticoagulated with ethylene diamine tetraacetic acid (EDTA), and centrifuged in plastic tubes at 2500 g for 25 min at 4 °C. The supernatant (plasma) was stored at − 20 °C until assays were performed. After OGD, rBMECs were cultured in media containing 10, 20, or 30% plasma concentrations. Ten percent plasma concentration was found to be optimal for cell proliferation after OGD ($p < 0.001$; data not shown), and used for group comparisons.

OGD in Human Umbilical Vein Endothelial Cells

Human umbilical vein endothelial cells (HUVEC) were harvested and cultured in 96-well cell culture plates evenly (15,000 cells per well), for 24 h. OGD was induced as above, and then cells were switched to high-glucose DMEM with EE or SC serum after MCAO, or SC serum after sham surgery, for 24 h. In a separate cohort, cell survival was measured without OGD, after incubation in high-glucose DMEM with EE or SC serum after MCAO, or SC serum after sham surgery, for 24 h. Cell survival was quantified as above. To obtain serum, blood samples were obtained by ventricular puncture 1 day after the 28-day housing intervention, allowed to clot, and centrifuged in plastic tubes at 2500 g for 15 min at 4 °C. The supernatant (serum) was stored at − 20 °C until assays were performed. After OGD, HUVEC were cultured in media containing 10% serum concentration for group comparisons.

Statistical Analysis

This was an exploratory study. Therefore, in the absence of prior data, sample sizes were selected based on anticipated variation aiming to achieve 80% power ($\alpha = 0.05$). Neurological deficit data and data on tissue outcome measures were obtained from separate cohorts. Because of higher than anticipated variation in the LSI data in EE group, a second EE cohort was added, doubling the sample size in this group. All data are expressed as whisker box plots (whiskers, full range; box, interquartile range; line, median; +, mean) or as mean ± standard deviation. Statistical analyses were performed using GraphPad Prism. Data were statistically tested using independent-samples *t* test, or one- or two-way ANOVA followed by Tukey's or Sidak's multiple comparisons test, as appropriate. Sample sizes are indicated in the text, on the figures and in the figure legends. Statistical tests are indicated in figure legends. $p < 0.05$ was considered statistically significant.

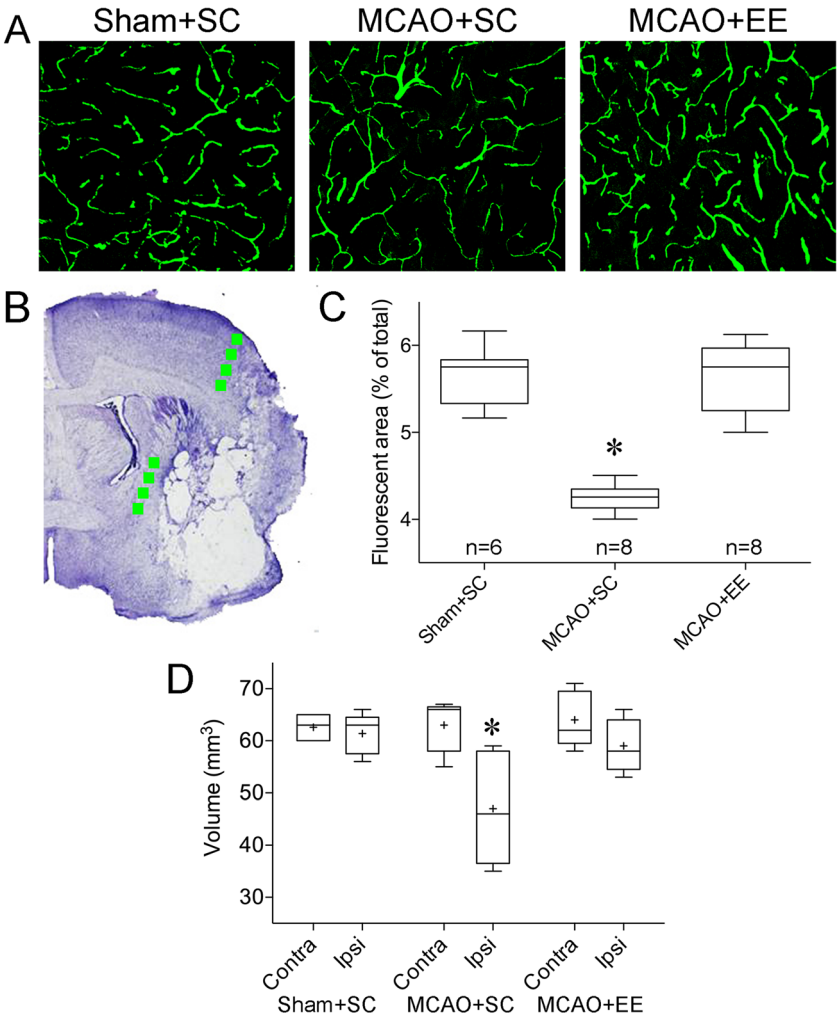

Fig. 2 Representative images (**a**; 200 × 200 μm) show microvascular fluorescence (**a**) in the ischemic border zone (**b**; eight ROIs within 1 mm of infarct edge) from sham, SC, and EE groups 15 days after MCAO. **c** Area of fluorescence was calculated as percentage of total image area as a measure of microvascular density ($n = 6$, 8, and 8 in Sham + SC, MCAO + SC, and MCAO + EE groups, respectively; $^*p < 0.0001$ vs. MCAO + EE and Sham + SC; one-way ANOVA followed by Tukey's multiple comparisons test). **d** Calculation of hemispheric atrophy in coronal sections (between bregma + 1.4 to + 4.8 mm) showed significantly preserved ipsilateral brain volume in the EE group ($n = 5$ each; $^*p < 0.05$ vs. MCAO + EE and Sham + SC; two-way ANOVA for repeated measures followed by Tukey's multiple comparisons test)

Results

Locomotor activity was two orders of magnitude higher in EE compared with SC rats ($n = 12$ each; Fig. 1b). At pre-ischemic baseline, EE and SC groups did not differ in foot fault test performance ($n = 7$ each). After MCAO, both groups exhibited worse scores, which persisted for at least 28 days (Fig. 1c). The deficits recovered faster and were consistently milder in the EE group compared with those in SC. The cylinder test also showed a strong trend towards better performance in the EE than SC group after MCAO ($n = 7$ each; $p = 0.08$; Fig. 1d). In a separate cohort, the SC group performed significantly worse in water maze test, compared with EE and sham groups ($n = 8$, 6, and 10, respectively; Fig. 1e–h). Although both EE and SC groups started with longer latencies to reach the correct quadrant after MCAO compared with sham, the EE group learned significantly faster than the SC group and was indistinguishable from sham controls on day 4 of the learning phase (Fig. 1f). During the probe test, the number of entries into and the time spent in the correct quadrant were significantly better in EE than SC rats (Fig. 1g, h).

Microvascular density in the peri-infarct region was higher in the EE group compared with that in SC, and comparable to sham controls (Fig. 2a–c). Indeed, volumetric assessment on coronal sections showed significantly less ipsilateral hemispheric atrophy in EE rats compared with SC (Fig. 2d).

In the sham group, cortical CBF values after sham surgery and 28 days later were comparable to baseline values ($1/k^2$ 1985 ± 216, 1843 ± 81, and 1984 ± 159, respectively; Fig. 3), confirming reproducible skull thinning and optical settings. One hour after MCAO, cortical CBF was significantly lower in the ischemic hemisphere compared to sham (51 ± 21 and 37 ± 16% of baseline; $p > 0.05$ SC vs. EE). There was a mild but consistent reduction in the contralateral hemisphere as well (71 ± 17 and 77 ± 17% of baseline, SC and EE, respectively; $p > 0.05$ SC vs. EE). Consistent with higher vascular density at 15 days, the EE group showed significantly higher cortical CBF values than SC in the ischemic hemisphere (108 ± 28 and 94 ± 16% of pre-ischemic baseline, respectively). Moreover, at 28 days, CBF appeared to increase even in the contralateral hemisphere in the EE group, while the SC group showed no change.

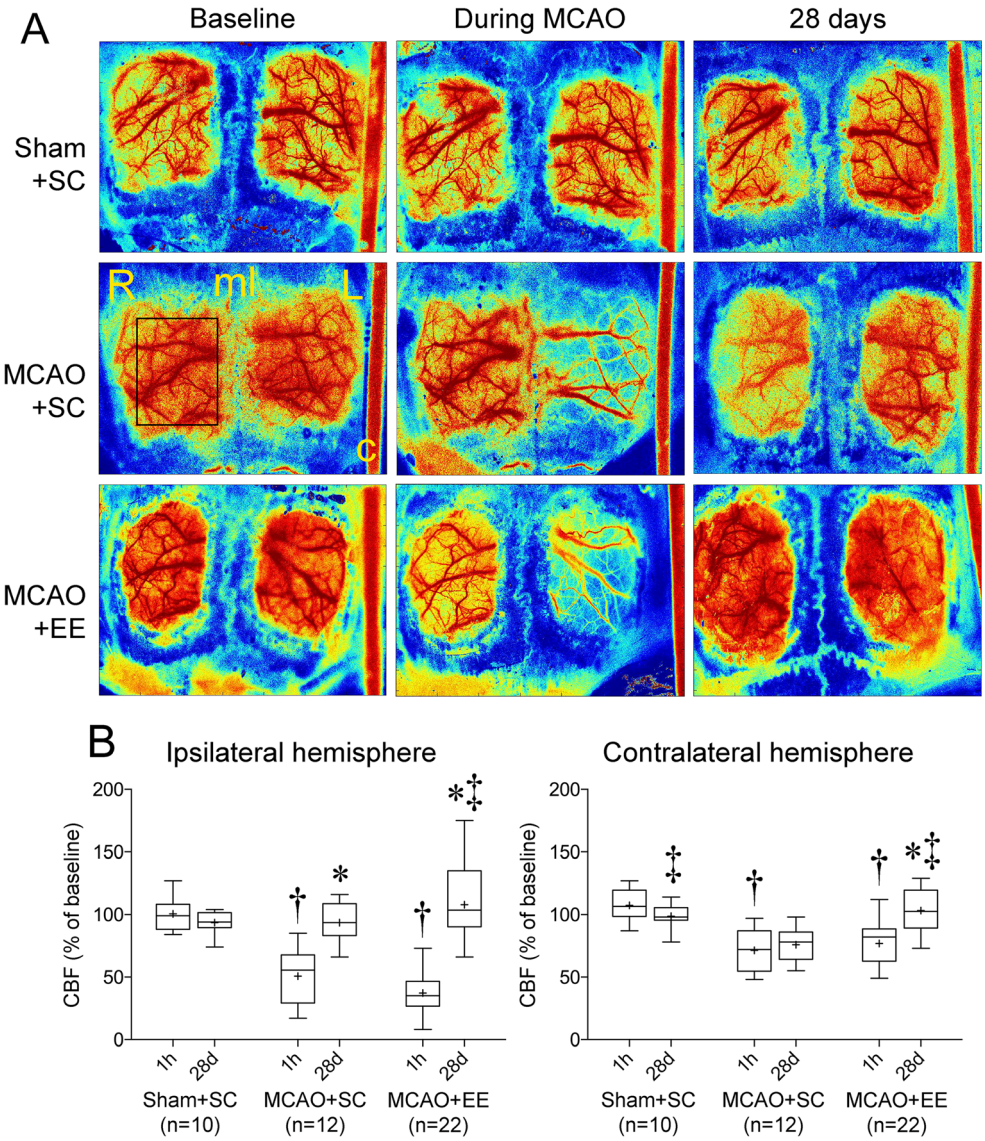

Fig. 3 Effect of enriched environment (EE) on cerebral blood flow (CBF) measured by laser speckle imaging. **a** Representative laser speckle images showing baseline, intra-ischemic (left MCAO) and 28-day CBF (R, right; L, left; ml, midline; c, catheter; rectangle, region of interest for CBF quantification) from Sham + SC, MCAO + SC, and MCAO + EE groups. Intra-ischemic CBF reduction in left hemisphere (during MCAO), and 28-day flow enhancement bilaterally in the MCAO + EE group are notable. **b** Summary data showing intra-ischemic (1 h) and 28-day post-ischemic CBF as percentage of pre-ischemic baseline, in Sham + SC, MCAO + SC, and MCAO + EE groups. EE augmented the 28-day CBF (†$p < 0.05$ vs. 1 h Sham + SC; ‡$p < 0.05$ vs. 28-day MCAO + SC; *$p < 0.05$ vs. 1 h; two-way ANOVA for repeated measures followed by Tukey's multiple comparisons test)

To test whether blood-borne factors may be responsible for the proangiogenic effect, we collected plasma or serum from EE or SC rats after MCAO or sham surgery. Plasma or serum from EE rats promoted the survival of both HUVEC (Fig. 4a) and rBMEC (Fig. 4b) compared with plasma (in rBMEC test) or serum (in HUVEC test) derived from the SC group after OGD. Importantly, serum from sham-operated SC, MCAO SC, and MCAO EE groups did not have a significant effect on HUVEC survival in the absence of OGD (OD 1.6 ± 0.1, 1.5 ± 0.1 and 1.5 ± 0.1, respectively; $n = 3$ each, $p = 0.75$). These data supported the hypothesis that systemic circulation can be a source for factors that promote revascularization after a transient focal ischemic insult. As a potential blood-borne candidate that can promote angiogenesis and inhibit apoptosis [29–31], we measured the serum and peri-infarct tissue levels of the potent proangiogenic factor HGF, and found them significantly higher in the EE group compared with those in SC when measured 15 days after stroke (Fig. 4c, d).

Discussion

Our data show that improved long-term neurological recovery by EE is associated with higher microvascular density and [32] CBF in peri-infarct brain tissue. We do not know whether the association is causal, or the identity of factors mediating the effect. However, the fact that post-stroke plasma or serum from EE rats significantly promoted rBMEC and HUVEC proliferation compared with plasma or serum from SC rats suggests the stimulus for enhanced angiogenesis may originate, at least in part, from the systemic circulation. In support of this notion, EE has also been shown to promote neurogenesis in aged rats via blood-borne factors [33]. HGF may be one such factor [34, 35]. HGF exerts its cellular effects via the c-Met receptor expressed on endothelial and vascular smooth muscle cells and coupled to cytoplasmic tyrosine kinase. HGF potently induces angiogenesis [36, 37], ameliorates cerebral endothelial apoptosis and ischemic neuronal injury [38, 39], preserves the blood–brain

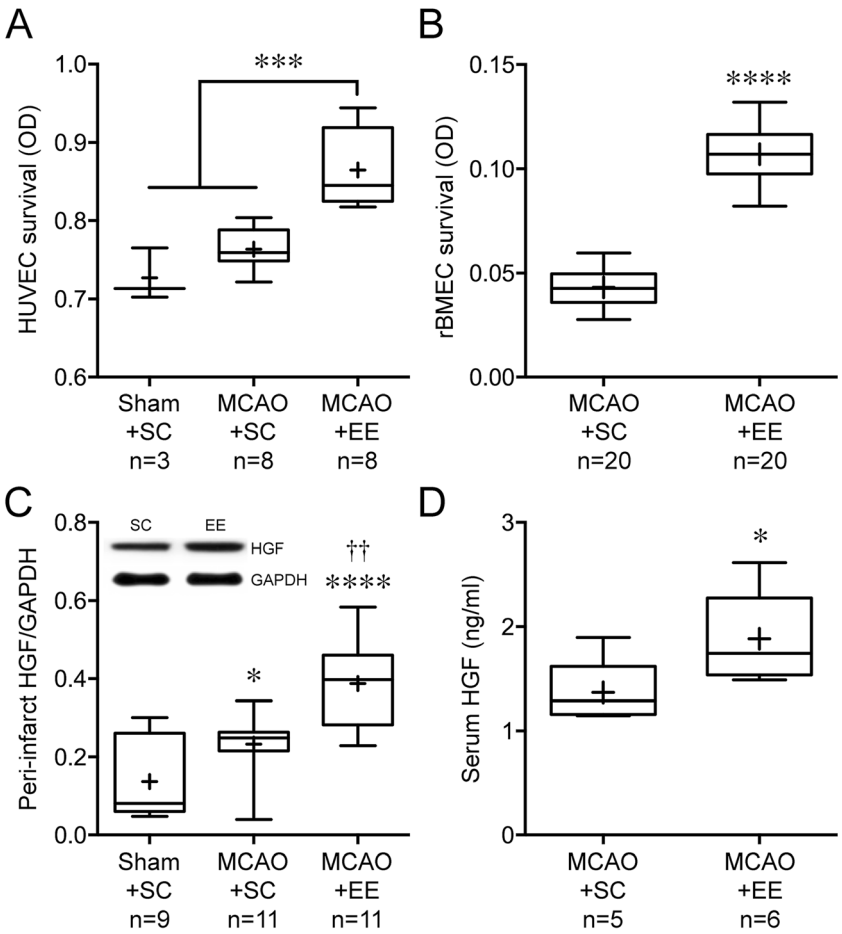

Fig. 4 The effect of plasma or serum on survival of **a** human umbilical vein endothelial cells (HUVEC; ***$p < 0.001$) and **b** rat brain microvascular endothelial cells (rBMEC; ****$p < 0.0001$) after oxygen-glucose deprivation, in vitro. **c** Ipsilateral cortical HGF levels (optical density, OD, of the HGF band was normalized to GAPDH; inset: representative bands; *$p < 0.05$, ****$p < 0.0001$ vs. Sham + SC; ††$p < 0.01$ vs. MCAO + SC). **d** Serum HGF levels (*$p < 0.05$; unpaired *t* test with Welch's correction)

barrier after cerebral ischemia [40], and facilitates stroke recovery [34, 41]. Moreover, a delayed increase in post-ischemic HGF levels has been reported, with a temporal profile suggestive of a role in tissue repair and recovery [42]. Therefore, increased peri-infarct HGF levels may in part explain the effect of EE on post-stroke angiogenesis. Indeed, HGF plasma levels are elevated in patients with ischemic stroke compared with healthy controls [43]. Of course, other major proangiogenic factors such as BDNF and VEGF are also likely to contribute, but whether they can also originate from plasma remains to be determined. More work is needed to directly link circulating HGF as a blood-borne factor promoting cerebral angiogenesis after stroke, and identify other potential blood-borne proangiogenic factors, such as VEGF [44, 45].

Improved stroke recovery upon EE correlates with the amount of voluntary exercise and physical activity [14]. Pre-ischemic exercise conditioning has been shown to facilitate angiogenesis [46], help preserve CBF during an ischemic insult [19, 47, 48], and alter multiple serum factors such as cytokines that can promote stroke recovery [47, 49–51]. Consistent with our data showing higher CBF in contralateral (i.e., non-ischemic) hemisphere in the EE group compared with the sham-operated SC group, EE has been shown to promote angiogenesis in a normal brain as well [52]. Besides improving the blood supply to the peri-infarct tissue, newly formed vessels provide trophic support to all cells within the neurovascular unit [53, 54], such as endothelial-oligodendrocyte trophic coupling [55, 56], thereby promoting plasticity, remodeling, and repair after stroke [57].

In conclusion, angiogenesis is an integral component of brain remodeling and functional recovery after stroke. Facilitating angiogenesis in surviving peri-infarct tissue may be a viable mechanism to promote recovery after stroke. Future work will focus on identifying the other circulating factors that are induced by EE and promote cerebral angiogenesis in return.

Author Contribution Statement YW, CA, and HX took part in conception and design; HX, KY, NZ, XS, ST, BZ, GL, JW, YW, CJ, CA, and RH took part in acquisition, analysis or interpretation of data; HX and KY contributed by drafting the article; YW and CA critically reviewed the article for intellectual content.

Funding This study was funded by the National Natural Science Foundation of China (NSFC, Grant nos. 81472150 and 81702218), Shanghai Municipal Commission of Health and Family Planning, Key developing disciplines (no. 2015ZB0401), the National Institutes of Health (NS055104), Foundation Leducq, Neuroendovascular Research Fund from the Andrew David Heitman Foundation, and The Ellison Foundation.

Compliance with Ethical Standards

Conflict of Interest Yi Wu has received research grants from the National Natural Science Foundation of China (NSFC, nos. 81472150) and Shanghai Municipal Commission of Health and Family Planning, Key developing disciplines (no. 2015ZB0401). Cenk Ayata has received research grants from the National Institutes of Health (NS055104), Foundation Leducq, Neuroendovascular Research Fund from the Andrew David Heitman Foundation, and The Ellison Foundation. Hongyu Xie has received research grant from the National Natural Science Foundation of China (NSFC, nos. 81702218) and declares that he has no conflict of interest. Kewei Yu declares that he has no conflict of interest. Naiyun Zhou declares that she has no conflict of interest. Xueyan Shen declares that she has no conflict of interest. Shan Tian declares that she has no conflict of interest. Bei Zhang declares that she has no conflict of interest. Yuyang Wang declares that he has no conflict of interest. Junfa Wu declares that he has no conflict of interest. Gang Liu declares that he has no conflict of interest. Congyu Jiang declares that he has no conflict of interest. Ruiping Hu declares that she has no conflict of interest. Cenk Ayata declares that he has no conflict of interest. Yi Wu declares that he has no conflict of interest.

Ethical Approval All applicable international, national, and/or institutional guidelines for the care and use of animals were followed.

References

1. Murphy TH, Corbett D. Plasticity during stroke recovery: from synapse to behaviour. Nat Rev Neurosci. 2009;10(12):861–72.
2. Dimyan MA, Cohen LG. Neuroplasticity in the context of motor rehabilitation after stroke. Nat Rev Neurol. 2011;7(2):76–85.
3. Iadecola C, Anrather J. Stroke research at a crossroad: asking the brain for directions. Nat Neurosci. 2011;14(11):1363–8.
4. Sutherland BA, Papadakis M, Chen RL, Buchan AM. Cerebral blood flow alteration in neuroprotection following cerebral ischaemia. J Physiol Lond. 2011;589(17):4105–14.
5. Beck H, Plate KH. Angiogenesis after cerebral ischemia. Acta Neuropathol. 2009;117(5):481–96.
6. Leventhal C, Rafii S, Rafii D, Shahar A, Goldman SA. Endothelial trophic support of neuronal production and recruitment from the adult mammalian subependyma. Mol Cell Neurosci. 1999;13(6):450–64.
7. Yamashita T, Ninomiya M, Acosta PH, Garcia-Verdugo JM, Sunabori T, Sakaguchi M, et al. Subventricular zone-derived neuroblasts migrate and differentiate into mature neurons in the post-stroke adult striatum. J Neurosci. 2006;26(24):6627–36.
8. Krupinski J, Kaluza J, Kumar P, Kumar S, Wang JM. Role of angiogenesis in patients with cerebral ischemic stroke. Stroke. 1994;25(9):1794–8.
9. Dahlqvist P, Ronnback A, Bergstrom SA, Soderstrom I, Olsson T. Environmental enrichment reverses learning impairment in the Morris water maze after focal cerebral ischemia in rats. Eur J Neurosci. 2004;19(8):2288–98.
10. Biernaskie J, Corbett D. Enriched rehabilitative training promotes improved forelimb motor function and enhanced dendritic growth after focal ischemic injury. J Neurosci. 2001;21(14):5272–80.
11. Nithianantharajah J, Hannan AJ. Enriched environments, experience-dependent plasticity and disorders of the nervous system. Nat Rev Neurosci. 2006;7(9):697–709.
12. Ekstrand J, Hellsten J, Tingstrom A. Environmental enrichment, exercise and corticosterone affect endothelial cell proliferation in adult rat hippocampus and prefrontal cortex. Neurosci Lett. 2008;442(3):203–7.
13. Longa EZ, Weinstein PR, Carlson S, Cummins R. Reversible middle cerebral-artery occlusion without craniectomy in rats. Stroke. 1989;20(1):84–91.
14. Xie HY, Wu Y, Jia J, Liu G, Zhang F, Zhang Q, et al. Enriched environment preconditioning induced brain ischemic tolerance without reducing infarct volume and edema: the possible role of enrichment-related physical activity increase. Brain Res. 2013;1508:63–72.
15. Van de Weerd HA, Aarsen EL, Mulder A, Kruitwagen CL, Hendriksen CF, Baumans V. Effects of environmental enrichment for mice: variation in experimental results. J Appl Anim Welf Sci. 2002;5(2):87–109.
16. Xie HY, Wu Y, Jia J, Liu G, Zhang Q, Yu KW, et al. Enrichment-induced exercise to quantify the effect of different housing conditions: a tool to standardize enriched environment protocols. Behav Brain Res. 2013;249:81–9.
17. Metz GA, Whishaw IQ. Cortical and subcortical lesions impair skilled walking in the ladder rung walking test: a new task to evaluate fore- and hindlimb stepping, placing, and co-ordination. J Neurosci Methods. 2002;115(2):169–79.
18. Vorhees CV, Williams MT. Morris water maze: procedures for assessing spatial and related forms of learning and memory. Nat Protoc. 2006;1(2):848–58.
19. Zhang PY, Yu HX, Zhou NY, Zhang J, Wu Y, Zhang YL, et al. Early exercise improves cerebral blood flow through increased angiogenesis in experimental stroke rat model. J Neuroeng Rehabil. 2013;10:43–53.
20. Bonner R, Nossal R. Model for laser Doppler measurements of blood flow in tissue. Appl Opt. 1981;20(12):2097–107.
21. Boas DA, Dunn AK. Laser speckle contrast imaging in biomedical optics. J Biomed Opt. 2010;15(1):1–12.
22. Dunn AK, Bolay H, Moskowitz MA, Boas DA. Dynamic imaging of cerebral blood flow using laser speckle. J Cereb Blood Flow Metab. 2001;21(3):195–201.
23. Zhang Q, Wu Y, Sha HY, Zhang PY, Jia J, Hu YS, et al. Early exercise affects mitochondrial transcription factors expression after cerebral ischemia in rats. Int J Mol Sci. 2012;13(2):1670–9.
24. Xie YC, Li CY, Li T, Nie DY, Ye F. Effect of mild hypothermia on angiogenesis in rats with focal cerebral ischemia. Neurosci Lett. 2007;422(2):87–90.
25. Abbott NJ, Hughes CCW, Revest PA, Greenwood J. Development and characterization of a rat-brain capillary endothelial culture-towards an in vitro blood–brain barrier. J Cell Sci. 1992;103:23–37.
26. Goldstein GW, Wolinsky JS, Csejtey J, Diamond I. Isolation of metabolically active capillaries from rat-brain. J Neurochem. 1975;25(5):715–7.
27. Arnaoutova I, George J, Kleinman HK, Benton G. The endothelial cell tube formation assay on basement membrane turns 20: state of the science and the art. Angiogenesis. 2009;12(3):267–74.
28. Tominaga H, Ishiyama M, Ohseto F, Sasamoto K, Hamamoto T, Suzuki K, et al. A water-soluble tetrazolium salt useful for colorimetric cell viability assay. Anal Commun. 1999;36(2):47–50.
29. Matsumoto K, Nakamura T. Emerging multipotent aspects of hepatocyte growth factor. J Biochem. 1996;119(4):591–600.
30. Nakamura T, Nishizawa T, Hagiya M, Seki T, Shimonishi M, Sugimura A, et al. Molecular-cloning and expression of human hepatocyte growth-factor. Nature. 1989;342(6248):440–3.
31. Zarnegar R, Michalopoulos GK. The many faces of hepatocyte growth-factor - from hepatopoiesis to hematopoiesis. J Cell Biol. 1995;129(5):1177–80.
32. Yu K, Wu Y, Zhang Q, Xie H, Liu G, Guo Z, et al. Enriched environment induces angiogenesis and improves neural function outcomes in rat stroke model. J Neurol Sci. 2014;347(1–2):275–80.
33. Villeda SA, Luo J, Mosher KI, Zou BD, Britschgi M, Bieri G, et al. The ageing systemic milieu negatively regulates neurogenesis and cognitive function. Nature. 2011;477(7362):90–4.

34. Chaparro RE, Izutsu M, Sasaki T, Sheng HX, Zheng Y, Sadeghian H, et al. Sustained functional improvement by hepatocyte growth factor-like small molecule BB3 after focal cerebral ischemia in rats and mice. J Cereb Blood Flow Metab. 2015;35(6):1044–53.
35. Doeppner TR, Kaltwasser B, ElAli A, Zechariah A, Hermann DM, Bahr M. Acute hepatocyte growth factor treatment induces long-term neuroprotection and stroke recovery via mechanisms involving neural precursor cell proliferation and differentiation. J Cereb Blood Flow Metab. 2011;31(5):1251–62.
36. Yang ZJ, Chen B, Sheng Z, Zhang DG, Jia EZ, Wang W, et al. Improvement of heart function in postinfarct heart failure swine models after hepatocyte growth factor gene transfer: comparison of low-, medium- and high-dose groups. Mol Biol Rep. 2010;37(4):2075–81.
37. Morishita R, Aoki M, Hashiya N, Yamasaki K, Kurinami H, Shimizu S, et al. Therapeutic angiogenesis using hepatocyte growth factor (HGF). Curr Gene Ther. 2004;4(2):199–206.
38. Van Belle E, Witzenbichler B, Chen DH, Silver M, Chang L, Schwall R, et al. Potentiated angiogenic effect of scatter factor/hepatocyte growth factor via induction of vascular endothelial growth factor—the case for paracrine amplification of angiogenesis. Circulation. 1998;97(4):381–90.
39. Miyazawa T, Matsumoto K, Ohmichi H, Katoh H, Yamashima T, Nakamura T. Protection of hippocampal neurons from ischemia-induced delayed neuronal death by hepatocyte growth factor: a novel neurotrophic factor. J Cereb Blood Flow Metab. 1998;18(4):345–8.
40. Date I, Takagi N, Takagi K, Kago T, Matsumoto K, Nakamura T, et al. Hepatocyte growth factor attenuates cerebral ischemia-induced learning dysfunction. Biochem Biophys Res Commun. 2004;319(4):1152–8.
41. Funakoshi H, Nakamura T. Hepatocyte growth factor (HGF): neurotrophic functions and therapeutic implications for neuronal injury/diseases. Curr Signal Transduction Ther. 2011;6(2):156–67.
42. Nagayama T, Nagayama M, Kohara S, Kamiguchi H, Shibuya M, Katoh Y, et al. Post-ischemic delayed expression of hepatocyte growth factor and c-met in mouse brain following focal cerebral ischemia. Brain Res. 2004;999(2):155–66.
43. Paczkowska E, Golab-Janowska M, Bajer-Czajkowska A, Machalinska A, Ustianowski P, Rybicka M, et al. Increased circulating endothelial progenitor cells in patients with haemorrhagic and ischaemic stroke: the role of endothelin-1. J Neurol Sci. 2013;325(1–2):90–9.
44. Kovesdi E, Gyorgy AB, Kwon SKC, Wingo DL, Kamnaksh A, Long JB, et al. The effect of enriched environment on the outcome of traumatic brain injury; a behavioral, proteomics, and histological study. Front Neurosci. 2011;5:1–12.
45. Ortuzar N, Rico-Barrio I, Bengoetxea H, Argandona EG, Lafuente JV. VEGF reverts the cognitive impairment induced by a focal traumatic brain injury during the development of rats raised under environmental enrichment. Behav Brain Res. 2013;246(1):36–46.
46. Ding Y, Li J, Luan X, Ding YH, Lai Q, Rafols JA, et al. Exercise pre-conditioning reduces brain damage in ischemic rats that may be associated with regional angiogenesis and cellular overexpression of neurotrophin. Neuroscience. 2004;124(3):583–91.
47. Zhang Q, Zhang L, Yang XJ, Wan YG, Jia J. The effects of exercise preconditioning on cerebral blood flow change and endothelin-1 expression after cerebral ischemia in rats. J Stroke Cerebrovasc Dis. 2014;23(6):1696–702.
48. Zwagerman N, Sprague S, Davis MD, Daniels B, Goel G, Ding YC. Pre-ischemic exercise preserves cerebral blood flow during reperfusion in stroke. Neurol Res. 2010;32(5):523–9.
49. Pedersen BK, Febbraio MA. Muscles, exercise and obesity: skeletal muscle as a secretory organ. Nat Rev Endocrinol. 2012;8(8):457–65.
50. Kohut ML, McCann DA, Russell DW, Konopka DN, Cunnick JE, Franke WD, et al. Aerobic exercise, but not flexibility/resistance exercise, reduces serum IL-18 CRP, and IL-6 independent of beta-blockers, BMI, and psychosocial factors in older adults. Brain Behav Immun. 2006;20(3):201–9.
51. Siqueira IR, Elsner VR, Rilho LS, Bahlis MG, Bertoldi K, Rozisky JR, et al. A neuroprotective exercise protocol reduces the adenine nucleotide hydrolysis in hippocampal synaptosomes and serum of rats. Brain Res. 2010;1316:173–80.
52. Bengoetxea H, Argandona EG, Lafuente JV. Effects of visual experience on vascular endothelial growth factor expression during the postnatal development of the rat visual cortex. Cereb Cortex. 2008;18(7):1630–9.
53. Lo EH. A new penumbra: transitioning from injury into repair after stroke. Nat Med. 2008;14(5):497–500.
54. Hamel E. Perivascular nerves and the regulation of cerebrovascular tone. J Appl Physiol. 2006;100(3):1059–64.
55. Miyamoto N, Pham LD, Seo JH, Kim KW, Lo EH, Arai K. Crosstalk between cerebral endothelium and oligodendrocyte. Cell Mol Life Sci. 2014;71(6):1055–66.
56. Arai K, Lo EH. An oligovascular niche: cerebral endothelial cells promote the survival and proliferation of oligodendrocyte precursor cells. J Neurosci. 2009;29(14):4351–5.
57. Liu YP, Lang BT, Baskaya MK, Dempsey RJ, Vemuganti R. The potential of neural stem cells to repair stroke-induced brain damage. Acta Neuropathol. 2009;117(5):469–80.